USING THE REVERSE PATH MULTI-INPUT-SINGLE-OUTPUT METHOD TO IDENTIFY NONLINEAR CHARACTERISTICS IN THE APPARENT MASS: PRELIMINARY RESULTS

Ya Huang
School of Engineering, University of Portsmouth
Portsmouth, PO1 3DJ, England
Ya.Huang@port.ac.uk

Abstract

The study implements a classic analysis technique in dynamics to examine nonlinear characteristics seen in apparent mass of a recumbent person during whole-body horizontal random vibration. The nonlinearity under present context refers to the amount of 'output' that is not correlated to the 'input' usually indicated by values of a coherence function that is less than unity. The analysis is based on longitudinal horizontal inline and vertical cross-axis apparent mass measured with 0.25-20 Hz random vibration at 0.125 and 1.0 ms^{-2} r.m.s. Adding the vertical cross-axis output force as a 'reversed' mathematical input markedly increased the multiple coherence of the apparent mass in the frequencies where ordinary coherence between the longitudinal horizontal excitation acceleration and the inline longitudinal force was low. Little improvement in the multiple coherence was achieved by an arbitrarily constructed mathematical input from the inline force.

1. Introduction

The paper outlines a system identification procedure to analyse 'paths' that contribute to nonlinear behaviours of biodynamic system such as the human body. The nonlinearity under present context refers to the amount of 'output' that is not correlated to the 'input' usually indicated by values of a coherence function that is less than unity. This mathematical nonlinearity is believed to associated with the biodynamic nonlinearity in which the resonance frequency increases with decreasing vibration magnitude (Huang and Griffin, 2008a, 2009). Improved understanding of the mathematical nonlinearity may help the definition and quantification of the biodynamic nonlinearity.

The biodynamic nonlinearity has been reported in both the vertical and the fore-and-aft responses of the seated human body during vertical whole-body vibration (Nawayseh and Griffin, 2003), in both the fore-and-aft and vertical responses of the seated human body during fore-and-aft whole-body vibration (Nawayseh and Griffin, 2003, 2005; Holmlund and Lundstrom, 2001), in both vertical and longitudinal horizontal responses of the recumbent person during vertical whole-body vibration (Huang and Griffin, 2008b), and in both longitudinal horizontal and vertical responses of the recumbent person during longitudinal horizontal whole-body vibration (Huang and Griffin, 2008a). With recumbent subjects, any voluntary or involuntary movement and muscular activity were eliminated. Therefore, it provided a better condition to examine linearity of a dynamic system comparing with other postures (Huang and Griffin, 2009).

The intended procedure is called reverse path nonlinear multi-input-single-output (MISO) method. It was introduced by Bendat (1992) and then more practically demonstrated with implementations by Bendat and Piersol (1993 and 2010). There are two principle steps: first, define and prepare

Presented at the 46th United Kingdom Conference on Human Response to Vibration, hosted by the Health and Safety Laboratory and the Health and Safety Executive, Buxton. 20-22nd September 2011

'mathematical' inputs (usually the measured output) and 'mathematical' output (usually the measured input) in the reverse path diagram (Figure 1); second, formulation of the MISO system including computation of frequency response functions (FRFs) based on correlated and uncorrelated mathematical inputs and their coherence functions (Figure 2).

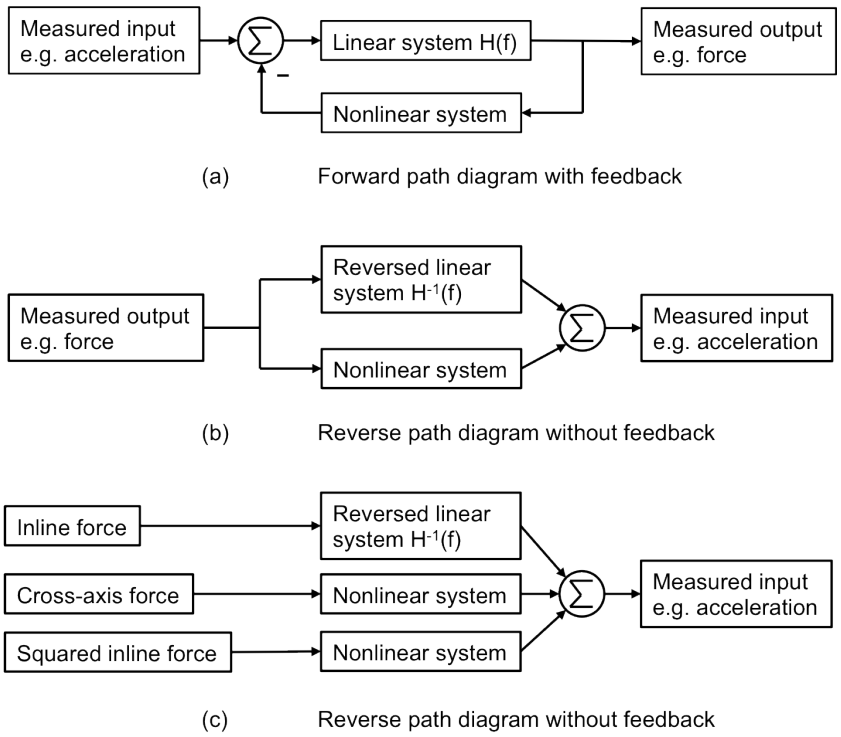

Figure 1 Reverse path diagram (a) derived from original forward path diagram (b), and (c) the implemented reverse path MISO system (adapted from Bendat and Piersol, 1993).

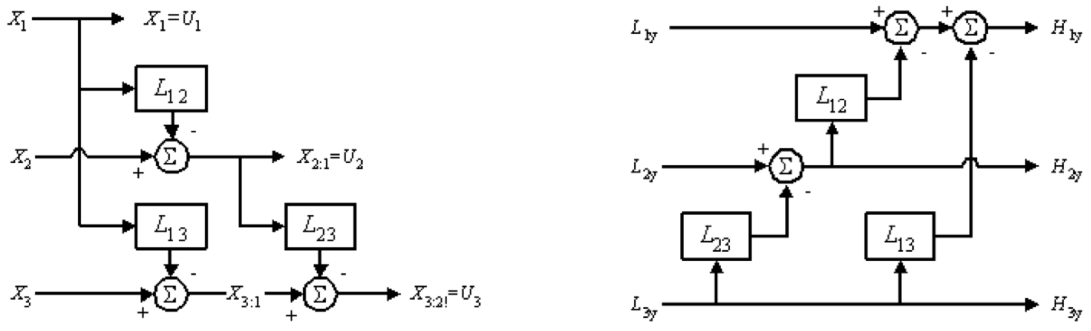

(a) Conditioned inputs 'U' (b) Recursive estimates of FRFs

Figure 2 (a) Conditioned or uncorrelated mathematical inputs (U_1, U_2, U_3) determined by recursive operation from correlated inputs (x_1, x_2, x_3). (b) FRFs of correlated inputs 'H' found from recursive sum of uncorrelated FRFs 'L' (Bendat and Piersol, 1993).

The full procedure has been used in structural dynamics to identify nonlinear behaviours presented in flexible and slender structures. A nonlinear stiffening effect of a beam structure clamped on its two ends was characterised by two nonlinear mathematical inputs in addition to the original dynamic force input (Sweitzer, 2006). The two added inputs were square and cubic of the input dynamic force. With the two mathematically constructed inputs, the multiple coherence function was markedly improved.

The MISO system was employed to analyse transmissibilites of multiple acceleration inputs during road-induced vehicle vibration (Qiu and Griffin, 2004). Instead of using arbitrarily constructed mathematical inputs, the authors used multiple channels of physical inputs – up to twelve accelerations at the four corners of the seat floor and each in the three orthogonal directions. The method identified the dominant channels of input acceleration in predicting the seat transmissibility.

With longitudinal horizontal random excitation of a semi-supine human body, the coherence function of the apparent mass showed a drop between 6 and 20 Hz (Huang and Griffin, 2008a). With increasing magnitude of excitation, the frequency of the coherence drop decreased – a similar behaviour to the resonance frequency of the apparent mass between 2 and 4 Hz. It was plausible to assume that at certain frequencies a part of the output force in the inline (longitudinal) direction was transferred to the cross-axis (vertical) direction, and therefore the coherence of the inline apparent mass was low at these frequencies. However, there has been no investigation to quantify the amount of 'transferred' output force from the inline axis to the cross axis.

In most biodynamic studies, any nonlinear effects were believed to be present in the 'output' side of the transfer function (e.g. Huang, 2007). It was not known whether the output could have a nonlinear feedback path to affect the linear input such as that shown in Figure 1a. At the same time, implementing a feedback loop in the frequency response functions (FRFs) involves time-consuming iterative procedures and stringent assumptions about the random distribution of the output. A reversed path would offer a more efficient computational algorithm for FRFs and coherences. The study examines the longitudinal inline and vertical cross-axis apparent mass of a supine body with 0.25-20 Hz random vibration at 0.125 and 1.0 ms^{-2} r.m.s. measured by Huang and Griffin, 2008a. The original system of input excitation and output force measured at the driving point was transformed into the reverse path diagram in Figure 1b. The longitudinal inline response force forms the first mathematical input, the vertical cross-axis force the second mathematical input, the square of the inline force the third mathematical input, and the longitudinal excitation acceleration the mathematical output (Figure 1c).

2. Method

While extensive procedures to derive uncorrelated (conditioned) mathematical inputs, correlated and uncorrelated FRFs, ordinary, partial and multiple coherence functions were demonstrated (Bendat and Piersol, 1993, 2010) and implemented (Qiu and Griffin, 2004; Sweitzer, 2006) elsewhere, The paper focuses on the key variables used to implement the method to examine the transfer function defined by apparent mass. The apparent masses of one semi-supine subject (S9) measured at two

magnitudes of continuous broadband random (0.25 to 20 Hz) vibration, i.e. 0.125 and 1.0 ms^{-2} r.m.s., were examined (data from Huang and Griffin, 2008a). Figures 3 to 6 are based on data of this experimental study. MATLAB 7.10 was used to perform all computational analysis.

The three mathematical inputs were defined from Figure 1 as:

x_1 – measured longitudinal inline response force at the driving point.

x_2 – measured vertical cross-axis response force at the driving point.

x_3 – constructed square of longitudinal inline response force at the driving point.

The one mathematical output was defined from Figure 1 as:

y – measured longitudinal excitation acceleration at the base.

In general, 'H' is used to denote transfer functions based on correlated original mathematical inputs, while 'L' for transfer functions based on conditioned or uncorrelated mathematical inputs where correlated portions are removed from each path. The general algorithm to formulate the MISO system in operational order is provided in Appendix A. The present study was based on three inputs and one output. A simplified notation is summarised below with a schematic representation shown in Figure 2.

Standard transfer function of apparent mass using cross spectral density (CSD) method takes the form: $H_1(f) = G_{oi}(f) / G_{ii}(f)$

$H_2(f) = G_{oo}(f) / G_{io}(f)$

and, for ordinary coherence function: $coh_{io} = | G_{io}(f) |^2 / (G_{ii}(f) G_{oo}(f)) = H_1(f) / H_2(f)$

where, $H_1(f)$ and $H_2(f)$ both measure the amount of output that is linearly correlated by the input; $H_1(f)$ assumes nonlinearity or noise comes from output; $H_2(f)$ assumes nonlinearity or noise comes from input; $G_{oi}(f)$ is the cross spectral density (CSD) function between the output and the input; $G_{ii}(f)$ and $G_{oo}(f)$ are the power spectral density (PSD) function for the input and the output; coh_{io} is the (ordinary) coherence function between the input and the output. In a normal sense, the input of the apparent mass is the excitation acceleration, output is the driving point dynamic force. However, as illustrated above, the reverse path method, the inputs will be constructed from the driving point dynamic force, i.e. x_1, x_2, and x_3, and the output will be the excitation acceleration, i.e. y.

The FRFs based on correlated original mathematical inputs i.e. H_{3y}, H_{2y}, and H_{1y} take the form:

$H_{3y} = L_{3y}$ where $L_{3y} = G_{3y:2!} / G_{33:2!}$

$H_{2y} = L_{2y} – L_{23} H_{3y}$ $H_{1y} = L_{1y} – L_{12} H_{2y} – L_{13} H_{3y}$

The FRFs based on uncorrelated conditioned mathematical inputs i.e. L_{2y}, L_{1y} are:

$L_{1y} = G_{1y} / G_{11}$

$L_{2y} = G_{2y:1} / G_{22:1}$

The ordinary coherence functions of conditioned inputs are:

$coh_{u1y} = (G_{y1} G_{1y}) / (G_{11} G_{yy})$ which is the same as the ordinary coherence function

$coh_{u2y} = (G_{y2:1} G_{2y:1}) / (G_{22:1} G_{yy})$

$coh_{u3y} = (G_{y3:2!} G_{3y:2!}) / (G_{33:2!} G_{yy})$

where subscript u denotes uncorrelated inputs, e.g. $u_1 = G_{11}$, $u_2 = G_{22.1}$, $u_3 = G_{33.2!}$, see Appendix A for $G_{jj.r!}$.

The multiple coherence functions as a summation of all uncorrelated contributions of inputs is:

$coh_{y:x} = coh_{u1y} + coh_{u2y} + coh_{u3y}$

In general there are two possible algorithms to compute the multiple coherence function (Bendat and Piersol, 1993). One is to compute the ordinary coherence functions of conditioned inputs as a percentage of the uncorrelated input u to the total output (G_{yy}) and then sum them up – described above. Another is to compute the partial coherence functions as a percentage of the uncorrelated input u but to the part of the output after removing the correlated contribution from the inputs ($G_{yy.(i-1)!}$) and then sum them up, see partial coherence in Appendix A. The first definition was used in the present study as the concept of ordinary coherence functions of conditioned inputs offers more physical interpretation of each uncorrelated input with regard to the overall output.

The linear FRF determined from the mathematical output y and the original mathematical input x_1 is

$H_{y1} = 1 / H_{1y}$

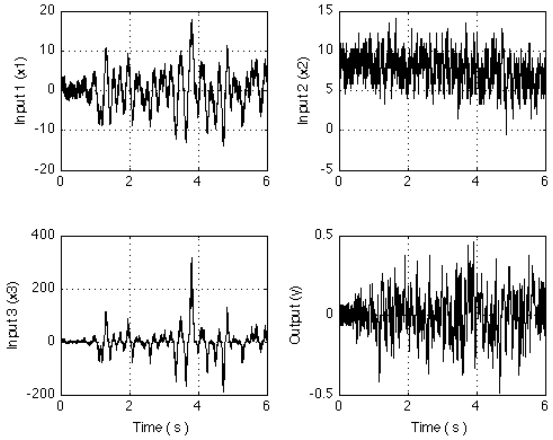

Figure 3 Time histories of the mathematical inputs: x_1 – horizontal inline output force at the driving point; x_2 – vertical cross-axis output force at the driving point; x_3 – squared horizontal inline force; and mathematical output: y – horizontal excitation acceleration at the base with each lasting for 90 seconds at 0.125 ms^{-2} r.m.s.

3. Results

The results are presented in the working order of the MISO recursive operation. Figure 4 shows the correlated and uncorrelated transfer functions and relevant coherence functions at 0.125 ms^{-2} r.m.s. The correlated (H) and uncorrelated (L) transfer functions show envelops inverse of the apparent

mass transfer function (H_1 and H_2 in Figure 6(a)) due to the reverse path algorithm. The main drop in the ordinary coherence (coh_{1y}) was between 12 and 20 Hz. Shown by its partial coherence (coh_{2y}), the second mathematical input (x_2), i.e. the cross-axis output force, exhibited improvement of up to 0.5 to the multiple coherence (coh_{yy}) in the frequency range of low coherence. At 0.125 ms^{-2} r.m.s., the cross-axis force also improved the ordinary coherence at lower frequencies near the primary resonance i.e. around 3, 4 and 7 Hz. The third mathematical input (x_3), i.e. the squared inline output force, had little contribution to the overall response.

At 1.0 ms^{-2} r.m.s., the main drop in the ordinary coherence (coh_{1y}) was between 8 and 16 Hz (Figure 5). The second mathematical input and its partial coherence coh_{2y} showed improvement of up to 0.7 to the multiple coherence (coh_{yy}) in this frequency range. There was small but evident improvement in the multiple coherence at lower frequencies near the primary resonance around 2 to 4 Hz. The third mathematical input had little contribution to the overall response. The drop in ordinary coherence was wider and greater at the high vibration magnitude than at the lower magnitude. In the frequency range of the main coherence drop, the cross-axis force improved the multiple coherence more at the higher magnitude of vibration than at the lower magnitude.

The difference between the two standard FRFs H1 and H2 in Figure 6 illustrated the frequency range at which the ordinary coherence function was low. In Figure 6, Hy1 represented the transfer function H(f) of the linear system in Figure 1(a) after removing effects from the nonlinear transfer functions H2y and H3y by means of calculating the uncorrelated transfer functions L1y and L2y. The primary resonance frequencies estimated by H1 and Hy1 were 3.8 and 3.9 Hz respectively at 0.125 ms-2 r.m.s., and 2.3 and 3.0 Hz respectively at 1.0 ms-2 r.m.s. (Figure 6). The primary resonance frequencies of Hy1 were estimated by curve fitting a 4-pole continuous time filter in the Laplace form to the FRF Hy1 using 'invfreqs()' in the MATLAB software. The difference between the resonance frequencies for H1 and Hy1 was larger at the higher vibration magnitude than at the lower magnitude.

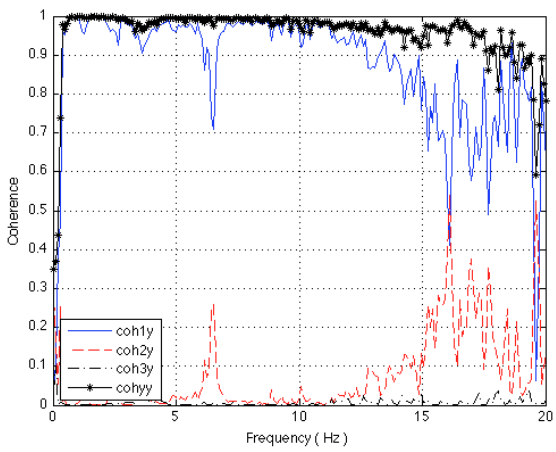

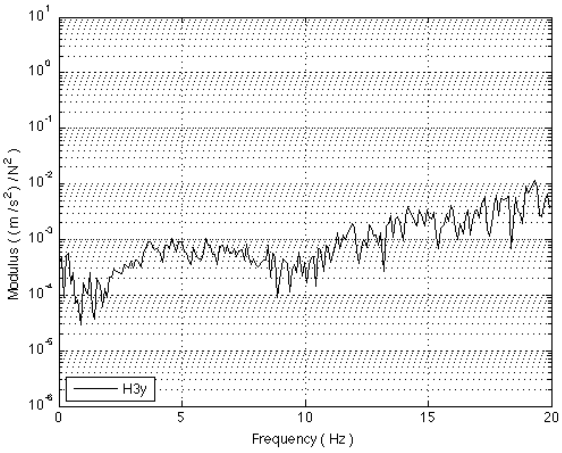

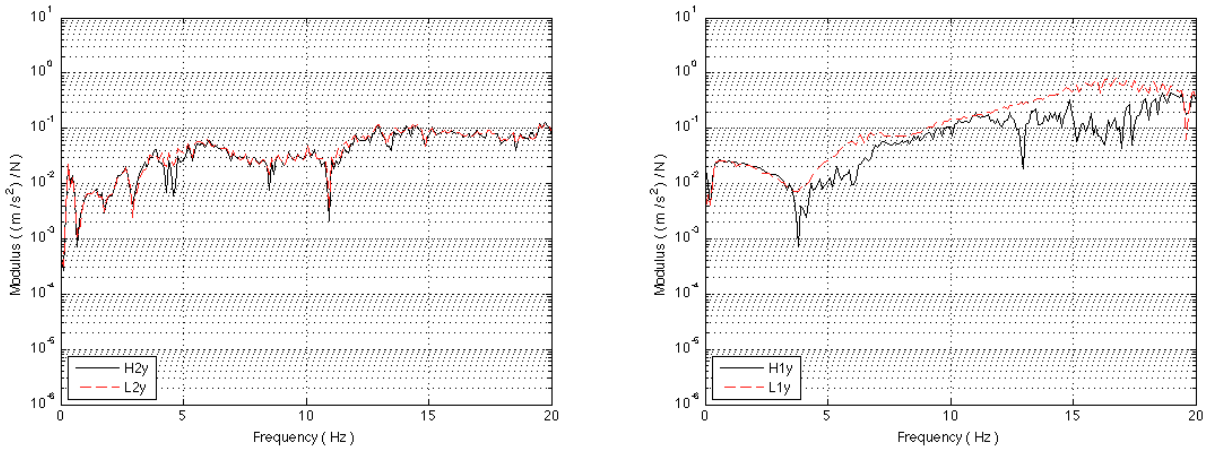

Figure 4 Ordinary coherence (coh_{1y}), partial coherence (coh_{2y}, coh_{3y}), and multiple coherence functions (coh_{yy}) computed based on individual and combined mathematical inputs (x_1, x_2, x_3) and output (y). H_{3y}, H_{2y}, H_{1y} – FRFs based on correlated mathematical inputs. L_{2y}, L_{1y} – FRFs based on uncorrelated mathematical inputs. Vibration magnitude: 0.125 ms^{-2} r.m.s., subject S9.

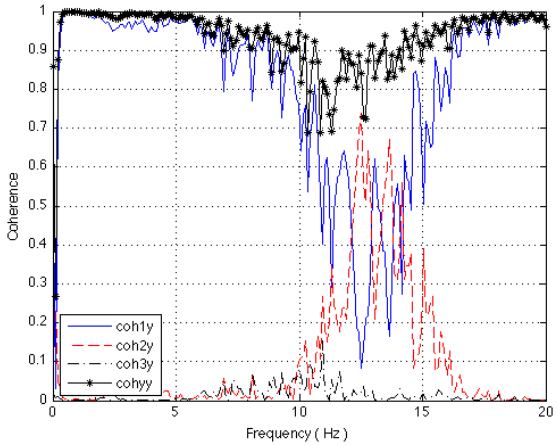

Figure 5 Ordinary coherence (coh_{1y}), partial coherence (coh_{2y}, coh_{3y}), and multiple coherence functions (coh_{yy}) computed based on individual and combined mathematical inputs (x_1, x_2, x_3) and output (y). Vibration magnitude: 1.0 ms^{-2} r.m.s., subject S9.

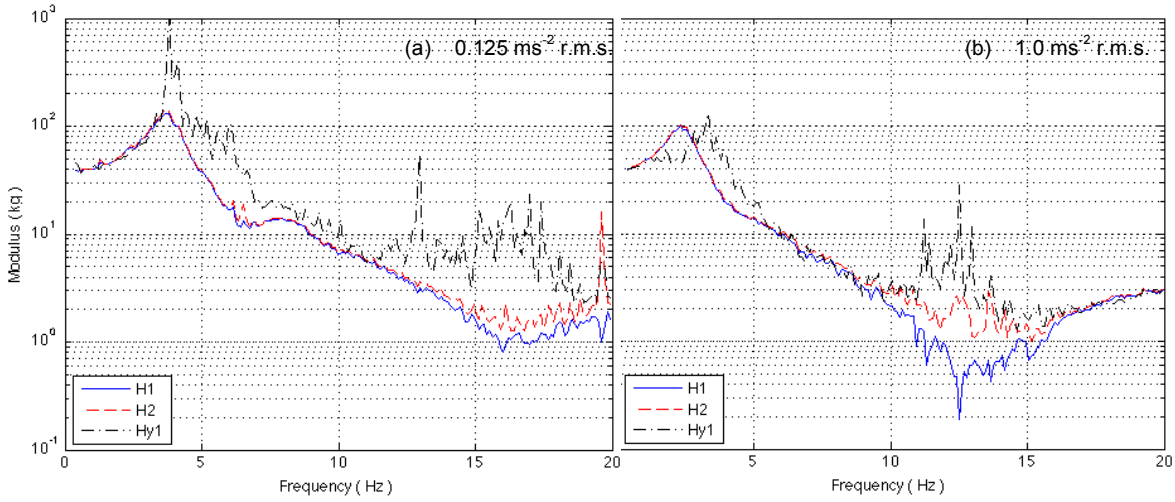

Figure 6 H_1 and H_2 are standard apparent mass FRFs. H_{y1} is the linear FRFs determined from the mathematical output y and mathematical input x_1. (a) Vibration magnitude 0.125 ms^{-2} r.m.s. (b) Vibration magnitude 1.0 ms^{-2} r.m.s. Subject S9.

4. Discussion and conclusions

Inclusion of the vertical cross-axis force response of the recumbent person effectively improve the coherence function measuring the linearity of the body system in the frequency range 8 to 18 Hz. Huang and Griffin (2008a) speculated that low output force at the driving point, or, high noise and distortion, at these frequencies could be the primary cause. Current study provided more quantitative explanation of the cause of the coherence drop in the horizontal apparent mass. However, in the frequency 8 to 18 Hz, some compensated coherences were still down to about 0.8 at 0.125 ms^{-2} r.m.s and down to about 0.7 at 1.0 ms^{-2} r.m.s. There must have been some other causes.

The constructed mathematical input (x_3) played little role in the multiple coherence function. Sweitzer (2006) applied mathematically constructed inputs to clamped beam structures where direction of movement was certain. The cross-axis movement of the recumbent human body introduced complexity when analysing the linearity or the nonlinearity of the body. Since any test condition involving human subject will be somehow affected by the cross-axis response, it would be plausible to explore means to eliminate or control such movements in the experiments. The reverse path MISO provides an alternative to investigate the linearity between signals. With better-controlled experiments, this method could be used to test effects of potential mathematical inputs on the linearity of the system. The mathematical inputs could be constructed by applying mathematical operations to physically measured input or output signals.

5. References

Bendat, J.S., Palo. P.A., and Coppolino, R.N. (1992). A general identification technique for nonlinear differential equations of motion. Probabilistic Engineering Mechanics 7, pages 43 – 61.

Bendat, J.S. and Piersol, A.G. (1993). Engineering Applications of Correlation and Spectral Analysis, 2nd Edition. John Wiley & Sons, Inc.

Bendat, J.S. and Piersol, A.G. (2010). Random Data: Analysis and Measurement Procedure, 4th Edition. John Wiley & Sons, Inc.

Holmlund, P. and Lundstrom, R. (2001). Mechanical impedance of the sitting human body in single-axis compared to multi-axis whole-body vibration exposure, Clinical Biomechanics 16 (Suppl. 1), S101–S110.

Huang, Y. (2007). Force harmonic distortion in the supine human body during vertical and longitudinal horizontal sinusoidal whole-body vibration. The 42nd United Kingdom Group Meeting on Human Responses to Vibration. 17 – 19 September 2007, Institute of Sound and Vibration Research, University of Southampton, Southampton, England,

Huang, Y. and Griffin, M.J. (2008a). Nonlinear dual-axis biodynamic response of the supine human body during longitudinal horizontal whole-body vibration. Journal of Sound and Vibration 312 (1–2), pages 273–295.

Huang, Y. and Griffin M.J. (2008b). Nonlinear dual-axis biodynamic response of the supine human body during vertical whole-body vibration. Journal of Sound and Vibration 312 (1–2), pages 296–315.

Huang, Y. and Griffin, M.J. (2009). Nonlinearity in apparent mass and transmissibility of the supine human body during vertical whole-body vibration. Journal of Sound and Vibration 324 (1–2), pages 429–452.

Nawayseh, N. and Griffin, M.J. (2003). Non-linear dual-axis biodynamic response to vertical whole-body vibration, Journal of Sound and Vibration 268, 503–523.

Nawayseh, N. and Griffin, M.J. (2005). Non-linear dual-axis biodynamic response to fore-and-aft whole-body vibration, Journal of Sound and Vibration 282, 831–862.

Qiu, Y. and Griffin M.J. (2004). Transmission of vibration to the backrest of a car seat evaluated with multi-input models. Journal of Sound and Vibration 274, pages 297–321.

Sweitzer, K.A. (2006). Random vibration response statistics for fatigue analysis of nonlinear structures. PhD thesis, University of Southampton, Southampton, UK.

Appendix A

General arithmetic for formulation of the MISO system (Bendat and Piersol, 1993)

Subscripts:

1, 2, 3 or x_1, x_2, x_3 – mathematical input

y – mathematical output

i, o – input and output

q – number of inputs

i, j – counter up to q

r – removed input channel number

r! – all input channels up to r

Recursive algorithm defined in Figure 2 is used to compute:

- conditioned single-sided auto and cross spectral density functions (e.g. G_{23});
- individual transfer functions between mutually uncorrelated (conditioned) inputs and the output (L_{iy});
- individual transfer functions between (usually correlated) original inputs and the output (H_{iy});
- ordinary and partial coherence functions ($coh_{iy:r!}$),
- multiple coherence functions (coh_{yi}).

Based on the recursive operations shown in Figure 2, arithmetic to formulate the MISO system can be performed in the following order (in the current study q = 3):

Conditioned PSDs and CSDs of relative to 2nd, 3rd until qth mathematical input

$$L_{rj} = G_{rj.(r-1)!} / G_{rr.(r-1)!} \qquad r = 1, \dots, (j-1);\ j = 1, \dots, q$$

$$G_{ij.r!} = G_{ij.(r-1)!} - L_{rj} G_{ir.(r-1)!} \qquad i > r,\ j > r,\ i \neq j$$

$$G_{jj.r!} = G_{jj.(r-1)!} - |L_{rj}|^2 G_{rr.(r-1)!} \qquad j > r$$

$$G_{iy.r!} = G_{iy.(r-1)!} - L_{ry} G_{ir.(r-1)!} \qquad i > r$$

$$L_{iy} = G_{iy.(i-1)!} / G_{ii.(i-1)!} \qquad i = 1, \dots, q$$

Partial coherence functions

$$coh_{iy.(i-1)!} = |G_{iy.(i-1)!}|^2 / (G_{ii.(i-1)!} / G_{yy.(i-1)!}) \qquad i = 1, \dots, q$$

$$G_{yi.r!} = G_{iy.(r-1)!} - L_{ri} G_{yr.(r-1)!} \qquad i > r$$

$$G_{yy.i!} = G_{yy.(i-1)!} - |L_{iy}|^2 G_{ii.(i-1)!} \qquad i = 1, \dots, q$$

Multiple coherence function with q inputs x.

$$coh_{y:q!} = 1 - (G_{yy.q!} / G_{yy}) = 1 - [(1 - coh_{1y}^2)(1 - coh_{2y.1}^2) \dots (1 - coh_{qy.(q-1)!}^2)]$$

Individual transfer functions of original inputs calculated from relations of conditioned inputs

$$H_{qy} = L_{qy}$$

$$H_{iy} = L_{iy} - \sum_{j=i+1}^{q} L_{ij} H_{jy} \qquad i = (q-1), (q-2), \dots, 1$$